Diagnostics of the prescriptions of death by a method of azimuthally-invariant Mueller-matrix microscopy

Ushenko, Alexander, Sarkisova, Yuliya, Bachinsky, Viktor, Vanchuliak, Oleg, Dubolazov, Alexander, et al.

Alexander G. Ushenko, Yuliya Sarkisova, Viktor T. Bachinsky, Oleg Y. Vanchuliak, Alexander V. Dubolazov, Yuriy O. Ushenko, Yuriy Y. Tomka, Roman M. Besaga, Konrad Gromaszek, Aigul Sagymbai, Adil Abdihanov, "Diagnostics of the prescriptions of death by a method of azimuthally-invariant Mueller-matrix microscopy," Proc. SPIE 11581, Photonics Applications in Astronomy, Communications, Industry, and High Energy Physics Experiments 2020, 115810J (14 October 2020); doi: 10.1117/12.2580335

Event: Photonics Applications in Astronomy, Communications, Industry, and High Energy Physics Experiments 2020, 2020, Wilga, Poland

Diagnostics of the prescriptions of death by a method of azimuthally-invariant Mueller-matrix microscopy

Alexander G. Ushenko*[a], Yuliya Sarkisova[b], Viktor T. Bachinsky[b], Oleg Y. Vanchuliak[b], Alexander V. Dubolazov[a], Yuriy O. Ushenko[a], Yuriy Y. Tomka[a], Roman M. Besaga[a], Konrad Gromaszek[c], Aigul Sagymbai[d], Adil Abdihanov[d]
[a]Chernivtsi National University, 2 Kotsiubynskyi Str., Chernivtsi, Ukraine, 58012; [b]Bukovinian State Medical University, 3 Theatral Sq., Chernivtsi, Ukraine, 58000; [c]Lublin University of Technology, Nadbystrzycka 38d, 20-618 Lublin, Poland; [d]L.N. Gumilyov Eurasian National University (ENU), Astana, Kazakhstan

ABSTRACT

The following paper presents research materials were presented: structural-logical scheme for diagnosing the limitation of death (AD) using the method of azimuthally invariant Mueller-matrix microscopy of the layers of the vitreous body (VB); temporal dynamics of necrotic changes of Mueller-matrix images (phase Mueller-matrix invariant (MMI)) of CT layers of the deceased; size and ranges of temporal changes in the statistical moments of the 1st to 4th orders characterizing the size distribution of images of the phase MMI of the layers of the VB of the deceased; effectiveness and accuracy of determining the AD by the method azimuthally invariant Mueller-matrix mapping layers VB decease.

Keywords: Mueller-matrix invariant, vitreous body, diagnostics

1. INTRODUCTION

Begin the Introduction two lines below the Keywords. The manuscript should not have headers, footers, or page numbers. It should be in a one-column format. References are often noted in the text[1] and cited at the end of the paper.

1.1 Structural-logical scheme for determining the ad by methods of azimuthally invariant polarization microscopy

Fig. 1 illustrates a structural-logical scheme for determining AD 1-3 by the method of azimuthally invariant Mueller-matrix microscopy:

Vitreous layer
Azimuthally invariant Mueller-matrix microscopy
Mueller-matrix mapping
Coordinate distribution of phase MMI
The temporal dynamics of changes in the statistical moments of the 1st - 4th orders, which characterize the coordinate distributions of the MMI of the vitreous body of the deceased in the postmortem period
The accuracy of determining the AD method Muller-matrix mapping of layers VB

Figure 1. Structural-logical scheme for determining AD by the method of azimuthally invariant Mueller-matrix microscopy.

1.2 The method of azimuth-invariant Mueller-matrix mapping of the layers of the vitreous body in the diagnosis of LD

Experimental measurements of azimuthally-invariant Mueller-matrix images (phase Mueller-matrix invariant - MMI) of CT preparations of the deceased with different AD were carried out according to the method, presented in detail in a series of scientific works [1, 2, 3].

The following groups of samples were investigated [4,5,6]:

- AD = 1 hour- group 1 (21 samples);
- AD = 3 hour - group 2 (21 samples);
- AD = 6 hour - group 3 (18 samples);

Photonics Applications in Astronomy, Communications, Industry, and High Energy Physics Experiments 2020
edited by Ryszard S. Romaniuk, Maciej Linczuk, Proc. of SPIE Vol. WI200, WI20000

- AD = 12 hour - group 4 (20 samples);
- AD = 18 hour - group 5 (22 samples);
- AD = 24 hour - group 6 (19 samples).

In Fig. 2 and fig. 3 shows maps (fragments (1)) and histograms (fragments (2), (3)) of the distributions of the magnitude of the phase MMI of polycrystalline fibrillar networks of VB layers of the dead from group 1 (AD 3 hours - Fig. 2) and group 3 (AD 12 hours - Fig. 3) [7,8,9].

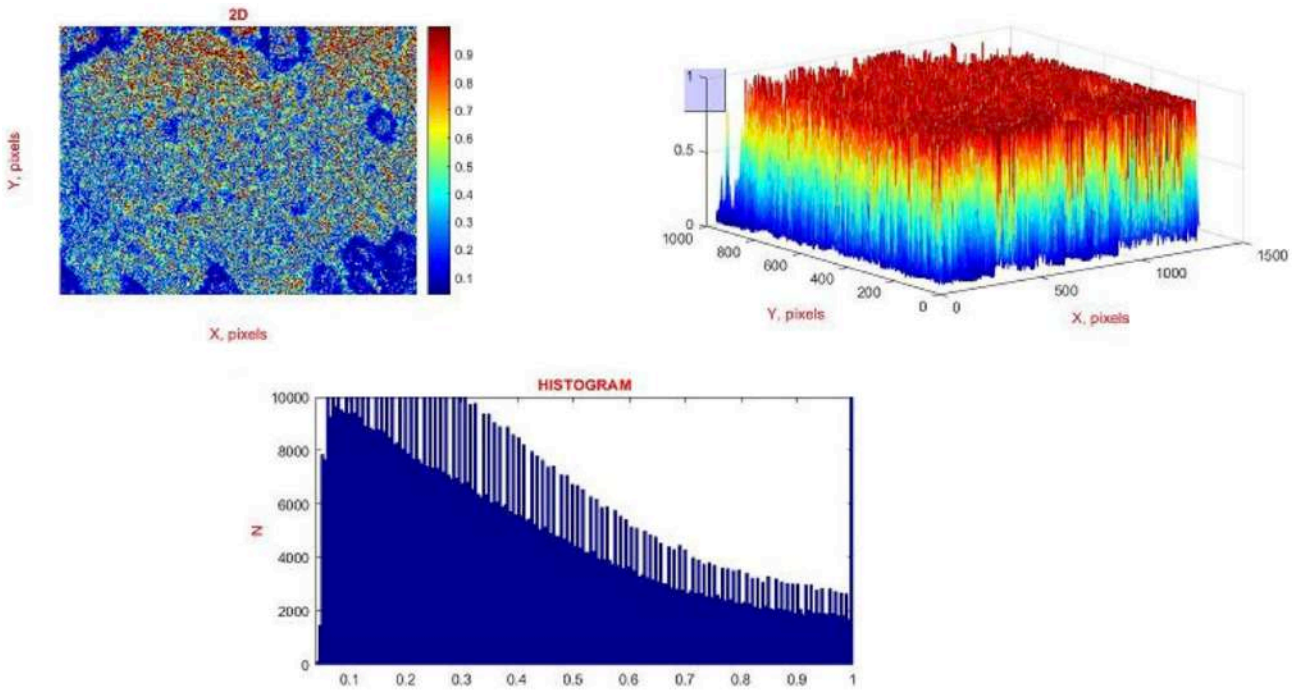

Figure 2. Maps (1) and distributions ((2), (3)) of the magnitude of the phase MMI VB layers of the deceased from AD 3 hours.

The results of the azimuthally-invariant Mueller-matrix mapping of the coordinate distributions of the magnitude of the phase MMI illustrate the presence of differences between the optical anisotropy of fibrillar collagen networks of VB layers of the deceased with different AD. It was revealed that the coordinate distributions of the magnitude of the phase MMI (Fig. 3, fragment (1)) of the sample layer VB (AD 12 hours). they are characterized by a large average magnitude and a range of scatter of random values compared to similar coordinate divisions of the phase MMI, determined by the VB of the deceased with AD 3 hours (Fig. 2, fragment (1)) [10,11,12] .

The established fact can be explained with the involvement of well-known literary data by the method of Muller-matrix mapping of histological sections of biological tissues of various human organs [10-14]. Here it is shown that the magnitude of optical anisotropy is inversely proportional to phase modulation at points in the plane of the VB layer (Fig. 2, Fig. 3, fragments (1)) [13,14,15].

Therefore, as AD increases, the level of optical anisotropy decreases due to necrotic changes [15,16,17].

In accordance with this, the depth of phase modulation of laser radiation by the optically anisotropic structures of sample VB is increased. Such a necrotic process corresponds to large random values of the phase MMI [7-13] .

As part of a statistical approach to analyzing the temporal dynamics of necrotic changes in maps of phase MMI VB layers of the deceased, AD growth is accompanied by opposite trends — an increase in the mean and variance characterizing the coordinate distribution of the phase MMI (Fig. 2, Fig. 3, fragments (2), (3)) [18,19,20].

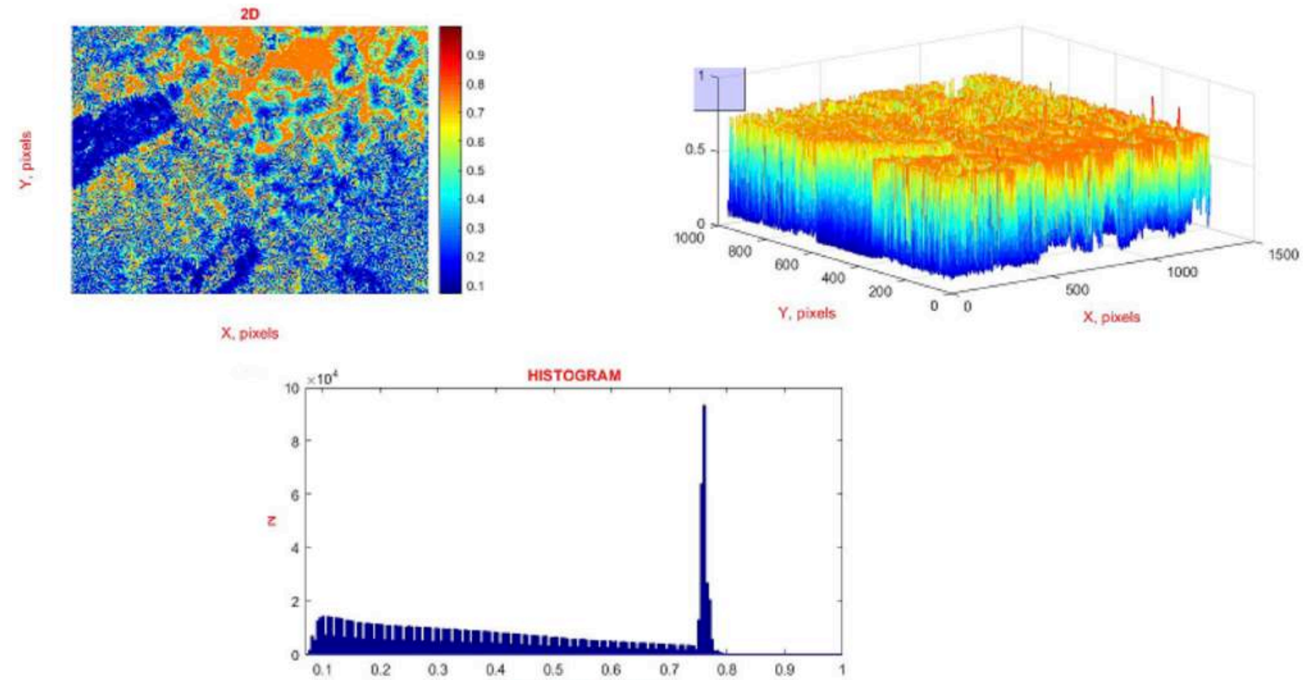

Figure 3. Maps (1) and distributions ((2), (3)) of the magnitude of the phase MMI VB layers of the deceased from AD 12 hours.

On the contrary, the values of the statistical moments of the 3rd and 4th orders, characterizing the asymmetry and excess of the coordinate distributions of the MMI value of polycrystalline structures of the VB layers of the deceased, decrease [22,23].

Quantitatively, this scenario of changes in the phase structure of fibrillar networks of VB samples of the deceased with different AD illustrates the statistical moments of the 1st - 4th orders given in Table 1 [24, 25, 31].

Table 1. Information The temporal dynamics of changes in the magnitude of the statistical moments of the 1st - 4th orders ($SM_{i=1,2,3,4}$), which characterize the distribution of the phase MMI.

SM_i	T=1	T=3	T=6	T=12	T=18	T=24
SM_1	$0{,}49 \pm 0{,}022$	$0{,}45 \pm 0{,}019$	$0{,}41 \pm 0{,}017$	$0{,}33 \pm 0{,}014$	$0{,}26 \pm 0{,}011$	$0{,}19 \pm 0{,}008$
p	$p \prec 0{,}05$	$p \prec 0{,}05$	$p \prec 0{,}05$	$p \prec 0{,}05$	$p \prec 0{,}05$	$p \prec 0{,}05$
SM_2	$0{,}27 \pm 0{,}012$	$0{,}25 \pm 0{,}011$	$0{,}22 \pm 0{,}01$	$0{,}17 \pm 0{,}008$	$0{,}13 \pm 0{,}006$	$0{,}09 \pm 0{,}004$
p	$p \prec 0{,}05$	$p \prec 0{,}05$	$p \prec 0{,}05$	$p \prec 0{,}05$	$p \prec 0{,}05$	$p \prec 0{,}05$
SM_3	$0{,}51 \pm 0{,}023$	$0{,}57 \pm 0{,}025$	$0{,}62 \pm 0{,}027$	$0{,}74 \pm 0{,}034$	$0{,}85 \pm 0{,}039$	$0{,}97 \pm 0{,}044$
p	$p \prec 0{,}05$	$p \prec 0{,}05$	$p \prec 0{,}05$	$p \prec 0{,}05$	$p \prec 0{,}05$	$p \prec 0{,}05$
SM_3	$0{,}61 \pm 0{,}027$	$0{,}65 \pm 0{,}029$	$0{,}72 \pm 0{,}033$	$0{,}87 \pm 0{,}038$	$1{,}01 \pm 0{,}045$	$1{,}19 \pm 0{,}052$
p	$p \prec 0{,}05$	$p \prec 0{,}05$	$p \prec 0{,}05$	$p \prec 0{,}05$	$p \prec 0{,}05$	$p \prec 0{,}05$

Established [27,28,29]:

- the linear range of variation of the magnitude of the 1st – 4th order statistical moments, which characterize the coordinate distributions of the magnitude of the phase MMI VB layers of the deceased in terms of AD, is 24 hours;

- the magnitude SM_1 varies within the range of averages determined for all groups of samples from 0.49 to 0.19,

- the magnitude SM_2 varies within the range of averages determined for all groups of samples from 0.27 to 0.09,

- the magnitude SM_3 varies within the range of averages determined for all groups of samples from 0.51 to 0.97,

- the magnitude SM_4 varies within the range of averages determined for all groups of samples from 0.61 to 1.19.

Fig. 4 illustrates linear charts of changes in the magnitude of a set of statistical moments.

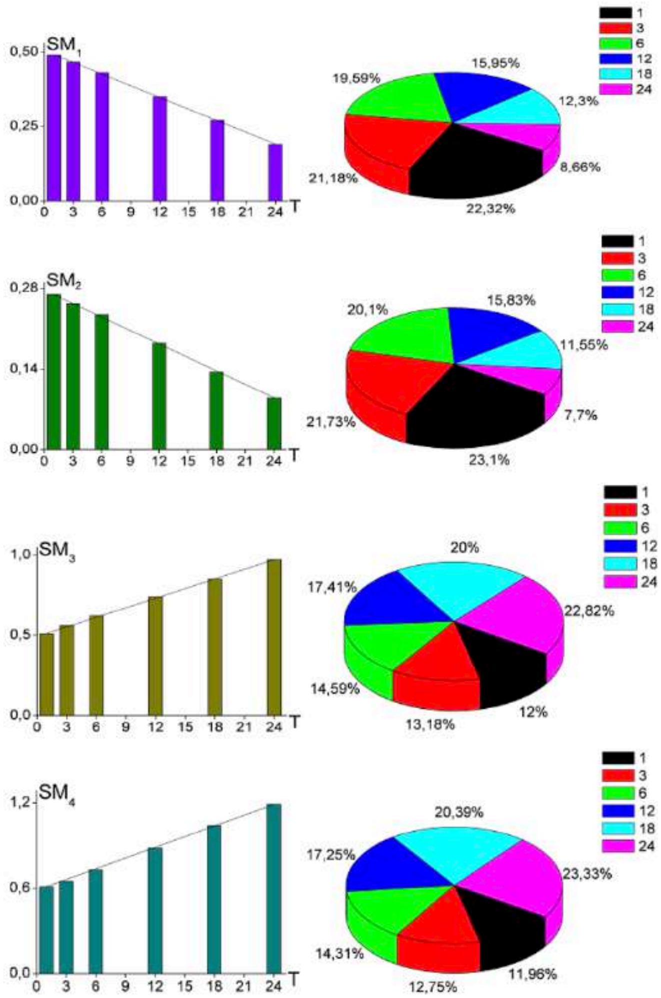

Figure 4. Temporal diagrams of changes in the magnitude of the statistical moments of the 1st - 4th orders ($SM_{i=1,2,3,4}$), which characterize the distribution of the phase MMI VB layers of the deceased with different AD (T, h).

From the data obtained (Fig. 4), it can be seen that the mean (1), dispersion (2), asymmetry (3) and excess (4) characterizing the maps of phase MMI VB layers of the deceased with different LD vary linearly within 24 hours. In this case, the most sensitive to the necrotic changes in the polycrystalline structure of such samples, as in the case of the method of azimuthally invariant polarization microscopy, were temporary changes in asymmetry and excess . Quantitatively, this is expressed in the growth of the angles of inclination of such linear dependences of the statistical moments of higher orders, - table 2.

Table 2. Information The temporal dynamics of changes in the magnitude of the statistical moments of the 1st - 4th orders ($SM_{i=1,2,3,4}$), which characterize the distribution of the phase MMI.

SM_i	T=1	T=3	T=6	T=12	T=18	T=24
SM_1	55 min.	56 min.	55 min.	57 min.	60 min.	61 min.
SM_2	52 min.	53 min.	52 min.	53 min.	53 min.	52 min.
SM_3	45 min.	46 min.	48 min.	47 min.	48 min.	48 min.
SM_3	44 min.	45 min.	44 min.	45 min.	45 min.	46 min.

Analysis of the obtained data on the time dependences of the magnitude of the statistical moments of the 1st – 4th order, characterizing the distribution of the magnitude of the phase MMI in different intervals of AD, found the maximum level (grayed out) in determining the AD within 44 min. - 46 min., Which is 5 min. better for polarization microscopy techniques [11,12,13].

CONCLUSION

The research presented in the article allowed to form the following conclusions:

1. A set of maps and histograms of the distributions of random values of the phase MMI VB layers of the dead with different limitation of death occurring was investigated by the method of azimuthally invariant Muller-matrix mapping;

2. The temporal dynamics of changes in the magnitude of the statistical moments of the 1st - 4th orders, characterizing the distribution of the magnitude of the phase MMI VB layers of the dead with different AD, was studied.

3. The sensitivity range (24 hours) and accuracy (45 min.) of the Mueller-matrix mapping of VB layers in certain AD were established.

REFERENCES

[1] Wang, X. and Wang, L.-H., "Propagation of polarized light in birefringent turbid media: a Monte Carlo study," J. Biomed. Opt. 7(1), 279-290 (2002).

[2] Tuchin, V. V., [Handbook of optical biomedical diagnostics], SPIE Press, Bellingham, 123–1110 (2002).

[3] Yao, G. and Wang, L. V., "Two-dimensional depth-resolved Muller matrix characterization of biological tissue by optical coherence tomography," Opt. Lett., 24(1), 537-539 (1999).

[4] Tower, T. T. and Tranquillo, R.T., "Alignment maps of tissues: I. Microscopic elliptical polarimetry," Biophys. J., 81(1), 2954-2963 (2001).

[5] Lu, S. and Chipman, R. A., "Interpretation of Muller matrices based on polar decomposition," J. Opt. Soc. Am. A., 13(1), 1106-1113 (1996).

[6] Ghosh, N. and Vitkin I. A., "Techniques for fast and sensitive measurements of two-dimensional birefringence distributions," Journal of Biomedical Optics., 16(11), 110795-110801 (2011).

[7] Tuchin, V. V. and Wang, L. and Zimnyakov, D. A., [Optical polarization in biomedical applications], New York, USA (2006).

[8] Ushenko, V.A., Koval, G.D., Gavrylyak, M.S., "Mueller - Matrices polarization selection of two-dimensional linear and circular birefringence images," Proceedings of SPIE - The International Society for Optical Engineering 8856, 88562E (2013)
[9] Prysyazhnyuk, V.P., Ushenko, Yu.A., Dubolazov, A.V., Ushenko, A.G. and Ushenko, V.A., "Polarization-dependent laser autofluorescence of the polycrystalline networks of blood plasma films in the task of liver pathology differentiation," Applied Optics 55(12), B126-B132 (2016)
[10] Ushenko, V. A., Sidor, M. I., Marchuk, Y. F., Pashkovskaya, N. V. and Andreichuk, D. R., "Azimuth-invariant mueller-matrix differentiation of the optical anisotropy of biological tissues," Optika i Spektroskopiya, 117(1), 152-157 (2014).
[11] Ushenko, V. A., Pavlyukovich, N.D., and Trifonyuk, L., "Spatial-frequency azimuthally stable cartography of biological polycrystalline networks," International Journal of Optics, 683168-683174 (2013).
[12] Ushenko, V. A., Zabolotna, N. I., Pavlov, S. V., Burcovets, D. M. and Novakovska, O. Yu., "Mueller-matrices polarization selection of two-dimensional linear and circular birefringence images," Proceedings of SPIE, 9066, 90661X (2013).
[13] Ushenko, V.O., "Two-dimensional mueller matrix phase tomography of self-similarity birefringence structure of biological tissues," Proceedings of SPIE, 8487, 84870W (2012).
[14] Smolarz, A., Gromaszek, K. and Wojcik, W., "Optical methods and artificial intelligence in diagnostics of industrial pulverized coal burner," Przeglad Elektrotechniczny, 88(9B), 259-261 (2012).
[15] Kotyra, A.; Wojcik, W. and Gromaszek, K. "Assessment of biomass-coal co-combustion on the basis of flame image," Przeglad Elektrotechniczny, 88(11B), 295-297 (2012).
[16] Rovira, R. H. Pavlov, S. V, Kaminski, O. S. and Bayas, M. M. "Methods of processing video polarimetry information based on least-squares and Fourier analysis," Middle-East Journal of Scientific Research, 16(9), 1201-1204 (2013).
[17] Zabolotna, N. I., Pavlov, S. V., Ushenko, A. G., Karachevtsev, A. O. and Savich, V. O., "System of the phase tomography of optically anisotropic polycrystalline films of biological fluids," Proc. SPIE 9166, 916616 (2014).
[18] Zabolotna, N. I., Pavlov, S. V., Ushenko, A. G., Sobko O. V. and Savich. V. O., "Multivariate system of polarization tomography of biological crystals birefringence networks," Proc. SPIE 9166, 916615 (2014).
[19] Kvyetnyy, R. N. Sofina O.Y. and Lozun, A. V., Smolarz A. and Zhirnova, O., "Modification of fractal coding algorithm by a combination of modern technologies and parallel computations," Proc. SPIE 9816, 98161R (2015).
[20] [20] Kvyetnyy, R. N., Bunyak, Y, Sofina, O., Kotyra, A., Romaniuk, R.S. and Tuleshova A. "Blur recognition using second fundamental form of image surface", Proc. SPIE 9816, 98161A (2015).
[21] [21] Roman N. Kvyetnyy, Olexander N. Romanyuk, Evgenii O. Titarchuk, Gromaszek, K. and Mussabekov N. "Usage of the hybrid encryption in a cloud instant messages exchange system", Proc. SPIE 10031, 100314S (2016).
[22] Tuzhanskyy, S. Y., "Methods and means of polarization parameter control in biotissue imaging polarimetry," Proc. SPIE 6682, 668212 (2007).
[23] Savenkov, S. N., Oberemok, Ye. A., Skoblya, Yu. A., Klimov, A. S. and Tuzhanskyy, S. Y., "Influence of imperfections of polarization elements on measurement errors in three probing polarizations method," Proc. SPIE 6164, 61640B (2006).
[24] Tuzhanskyi, A. Y., Sakhno, A. M., Komada, P., Kashaganova, G. and Smolarz, A., "Fiber optic gyroscope based on the registration of the spatial interference pattern," Proc. SPIE 9816, 98160Z (2015).
[25] Nosova, Y., Shushliapina, N., Kostishyn, S. V., et al., "The use of statistical characteristics of measured signals to increasing the reliability of the rhinomanometric diagnosis," Proc. SPIE 10031, (2016).
[26] Kozlovska, T. I., Kolisnik, P. F., Zlepko, S. M., et al., "Physical-mathematical model of optical radiation interaction with biological tissues," Proc. SPIE 10445, (2017).
[27] Kozlovska, T. I. and Pavlov. S. V., [Optoelectronic means of diagnosing human pathologies associated with peripheral blood circulation], LAP LAMBERT Academic Publishing, Beau Bassin 71504, Mauritius, 1-59 (2019).
[28] Dubolazov, O. V., Ushenko, A. G., Pavlov, S. V. and etc., "The complex degree of coherence of the laser images of blood plasma and the diagnostics of oncological changes of human tissues," Information Technology in Medical Diagnostics II. CRC Press, Taylor & Francis Group, London, 185-194 (2019).
[29] Dubolazov, O. V. Ushenko, A. G., Ushenko, Y. A., Sakhnovskiy, M. Yu., Grygoryshyn, P. M., Pavlyukovich, N., Pavlyukovich, O. V., Bachynskiy, V.T., Pavlov, S. V., Mishalov, V. D., Omiotek Z. and Mamyrbaev, O.,

"Laser Müller matrix diagnostics of changes in the optical anisotropy of biological tissues," Information Technology in Medical Diagnostics II., CRC Press, Taylor & Francis Group, London, 195-203 (2019).
[30] Dubolazov, O. V., Ushenko, A. G., Pavlov, S. V. and etc., "Laser microscopy of polycrystalline human blood plasma films," Information Technology in Medical Diagnostics II., CRC Press, Taylor & Francis Group, London, 205-217 (2019).
[31] Rovira, R. H., Pavlov, S. V., Wójcik W. and etc., "Tele-detection system for the automatic sensing of the state of the cardiovascular functions in situ," Information Technology in Medical Diagnostics II, CRC Press, Taylor & Francis Group, London, 289-296 (2019).N. and Smith, A. S., [Infrared Detectors], Goodwin House Publishers, New York & Boston, 241-248 (1997).